Sensors and Materials, Vol. 34, No. 5 (2022) 2007–2013
MYU Tokyo

S & M 2950

Optoelectronics Inspection of Amorphous In–Ga–Zn–O-based Active-matrix Thin-film Transistor Array for Foldable Substrate Applications

Shih-Hung Lin,[1†] Chi-Hang Siu,[2†] Yuan-Ting Wang,[3] and Yao-Chin Wang[4*]

[1]Department of Electronics Engineering, National Yunlin University of Science and Technology, 123, University Road, Section 3, Douliou, Yunlin 64002, Taiwan
[2]Department of Critical Care Medicine and Department of Surgery, Kuang Tien General Hospital, 117, Shatian Road, Shalu District, Taichung City 43303, Taiwan
[3]Tainan First Senior High School, 1, Sec. 1, Mintzu Road, Tainan City 701005, Taiwan
[4]Department of Computer Science and Information Engineering, Cheng Shiu University, 840, Chengcing Road, Niaosong District, Kaohsiung City 83347, Taiwan

(Received March 31, 2022; accepted May 12, 2022)

Keywords: inspection, IGZO, thin-film transistor, foldable device

In this study, we report the flaw detection properties of amorphous In–Ga–Zn–O (IGZO)-based active-matrix thin-film transistors (TFTs) on foldable device applications. Thinned-glass and foldable substrates are two different types of critical flexible substrate for defect inspection, which are also difficult to check by traditional in situ inspection techniques for mass production. The technique we proposed is based on the noninvasive optoelectronic transforming principle to inspect flaw pixels, with the advantages of an ultrahigh resolution, a small pixel array, and no contact damage. This method can be applied to foldable substrates with an ultrahigh-definition (UHD) TFT array panel and digital X-ray detectors. The experimental data showed good flaw detection rate (>90.1%) and fail detection rate (<4.9%).

1. Introduction

Recently, amorphous In–Ga–Zn–O (IGZO)-based thin-film transistor (TFT) pixels have been successfully used in advanced and ultrahigh-resolution display backplanes (Figs. 1 and 2). Park *et al.*[(1)] reported an application of a full-color flexible organic light-emitting diode (OLED) display driven by an amorphous IGZO TFT on a polyimide (PI) plastic substrate. They mentioned the fabrication of a 6.5-inch full-color flexible top-emission active-matrix OLED display on a PI substrate, driven by amorphous IGZO TFTs. Mo *et al.*[(2)] presented a 12.1-inch-wide extended graphics array (WXGA) active-matrix OLED display; they illustrated the display using IGZO-TFTs as an active-matrix backplane. Nam *et al.*[(3)] proposed a 65-inch OLED television using IGZO TFTs with W/R/G/B pixel design.

High-quality, high-reliability, and good-performance panels need to be manufactured for customers. A TFT inspection system has been widely used for providing flaw detection

*Corresponding author: e-mail: y.c.wang@ieee.org
†These authors equally contributed to the paper.
https://doi.org/10.18494/SAM3911

ISSN 0914-4935
https://myukk.org/

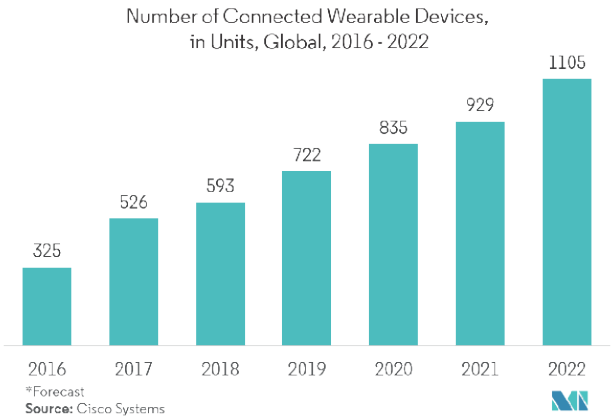

Fig. 1. (Color online) Global IGZO market forecast for connected wearable devices (https://www.mordorintelligence.com/industry-reports/indium-gallium-zinc-oxide-market).

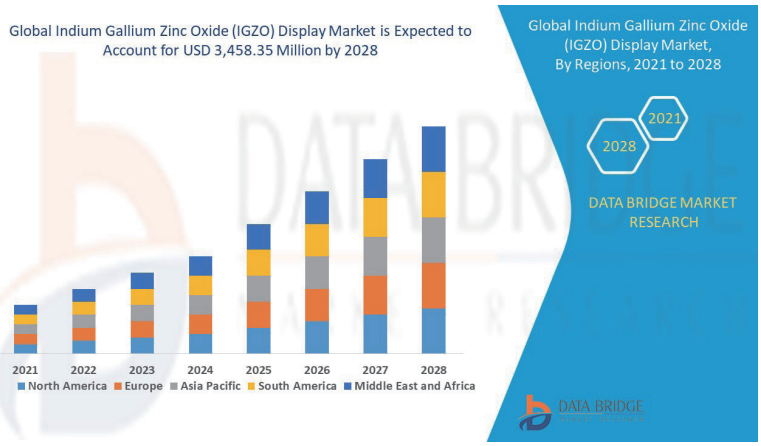

Fig. 2. (Color online) Global IGZO display market forecast (2021 to 2028) (https://www.databridgemarketresearch.com/reports/global-indium-gallium-zinc-oxide-igzo-display-market).

capability with in situ process checking.[4] With cost reduction and increasing yield in advanced ultrahigh-resolution display panels, flaw detection is becoming a high priority for manufacturers of displays for small-pixel-sized applications.[5]

Over the past years, a number of technologies have been developed and applied for the inspection of defects on TFT arrays,[6–11] but Liu did not mention how to detect flaw pixels with TFT characterization.[6,10] Kido *et al.*[7] faced an unstable charge density issue with optical sensing sensitivity and showed the limitation of detecting critical defects in small pixel sizes. The electron beam technique[8] is used to inspect and detect a few types of flaw. However, it requires a long working time for operation and also a high stability of the instruments. The testing by electrical schemes[9,11] requires many contact pins on a substrate for direct contact and measurement, which also require a long preparation time and a high cost for production. In

summary, they did not propose how to inspect critical small-pixel flaws on thinned-glass and foldable substrates.

We showed that the proposed technique was for detecting flaws on advanced medical display panels[4] because of the above issues. The technique was used for detection by optoelectrical conversion with TFT characterization. It provides good detection rate of small-pixel-sized TFTs with the advantages of in-process high-precision testing and array inspection and managing the yield of the TFT array process in manufacturing.[12,13]

Because of the TFT's behavior and characteristics, we reported and detected amorphous IGZO-based active TFT critical pixel flaws and showed the flaw position in panels. We measured these characteristics of devices, which provided information on how good is the TFT array. The results showed and provided a good solution for small-pixel flaw detection, especially in ultrahigh-resolution display applications such as small-sized α-IGZO TFT pixels.

2. Experimental Methods

In this section, we discuss the materials for the technique using the developed inspection system for flaw detection. Figure 3 shows the subpixel and R/G/B square pixel of amorphous IGZO-based active TFTs. Under electrical stress, amorphous IGZO-based oxide TFT pixels have attracted considerable attention owing to their advantages such as smaller subthreshold swing, higher field effect mobility, higher uniformity, higher resolution applications, and higher stability than amorphous silicon TFT pixels.

Normally, an active pixel TFT device is arranged from the surrounding TFTs and is served by an electrode of one capacitor. The illustrated 2D TFT array pixels were fabricated on glass or flexible substrates. The gate lines are connected parallel to the other gates of the next TFTs. The data lines are series-connected to the drain and source terminals of the TFTs. Both the gate and data lines comprised one set of vertical metal lines and one set of horizontal metal lines on TFT panels. Generally, the TFT devices on display panels also consist of a two-dimensional array of controlled pixels. The source and drain terminals are connected to a transparent conductor with another TFT pixel. Figure 4 shows how to detect a flaw on a pixel with the driving pattern.

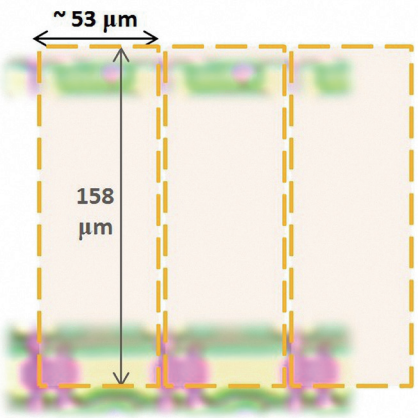

Fig. 3. (Color online) Subpixel and R/G/B square pixel of amorphous IGZO-based active TFTs.

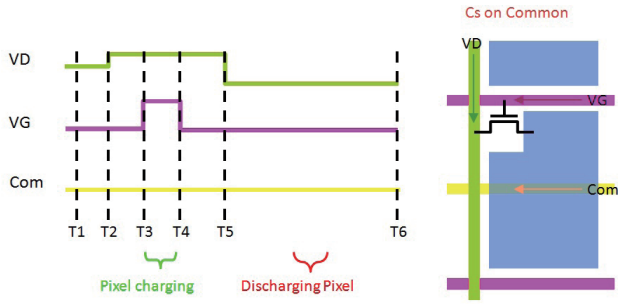

Fig. 4. (Color online) Driving pattern showing how to detect a flaw on a pixel. (Ex. Cs on Common)

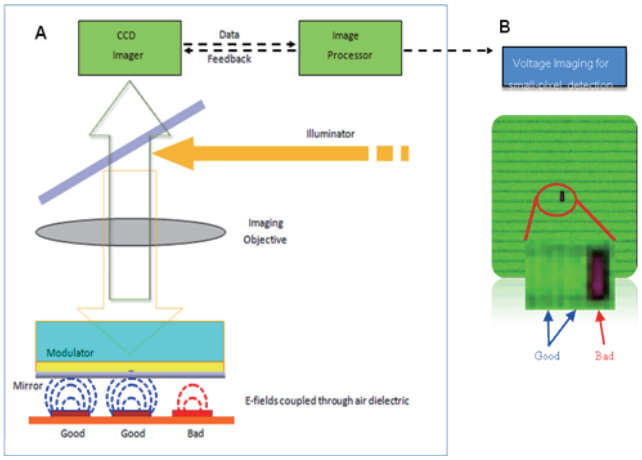

Fig. 5. (Color online) Basic operation theory and measurement.

T1: TFT switch off, VD = 0 V
T2: TFT switch off, VD = driving voltage
T3: TFT switch on, VD = driving voltage (Pixel charging)
T4: TFT switch off, VD = driving voltage
T5: TFT switch off, VD = driving voltage
T6: CCD camera trigger for flaw map (8.6 ms for 60 frames per second)

Herein, the flaw pixel voltage drop was caused by pixel charging. In this report, *VN* is the measured voltage of the normal pixel (= *VD*).[12,13]

Figure 5 shows the basic operation theory of optoelectrical transformation with TFT characterization. The sensing modulator will sense the voltage induced by the pixels' E-fields. Figure 5 also shows the measured pixel voltage; green is for good pixels and dark is for bad pixels.

3. Results and Discussion

The flaw map in Fig. 6(a) shows the detected flaw pixels of zooms 1 and 2. In zoom 2, we see flaws very clearly on the flaw map. The optical microscopy images in Fig. 6(b) show real flaws

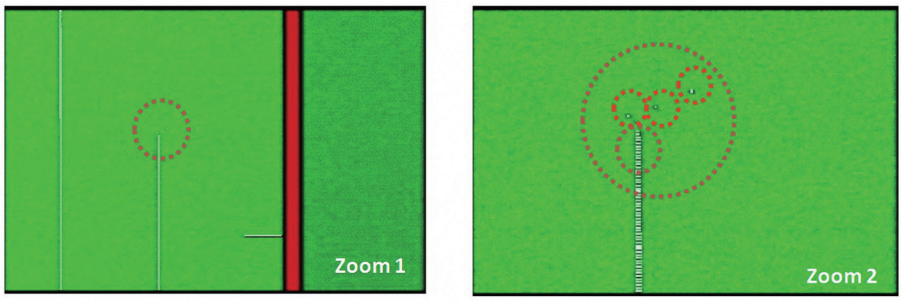

(a)

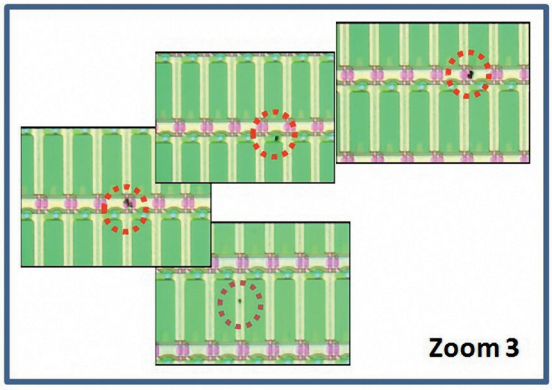

(b)

Fig. 6. (Color online) (a) Flaw map showing the detected flaw pixels of zooms 1 and 2. (b) Flaw map and optical microscopy images.

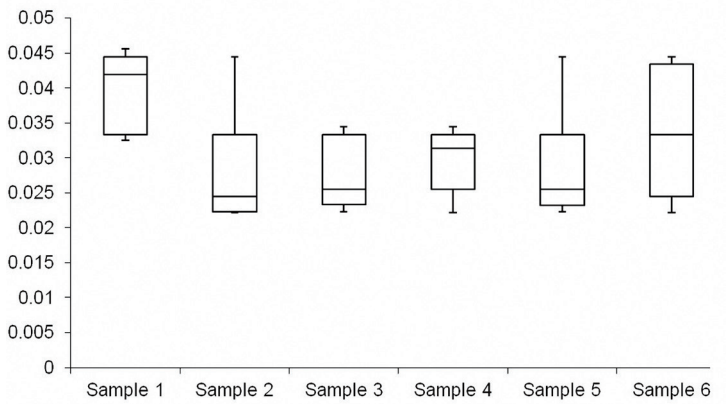

Fig. 7. Six samples of measured flaw pixels: fail detection <5% and stable uniformity also <5%.

on pixels. After the testing was completed, the uniformity of the test data as the failure detection rate was shown (Fig. 7). Table 1 shows the limitation of some flaws that can and cannot be detected.

Table 1
Limitation of some flaws that can and cannot be detected.

Defect type	Detection
Gate-to-data short	Partial
Gate-to-gate short	Partial
Date-to-data short	Partial
Gate line open	Yes
Date line open	Yes
TFT pixel open	Yes

4. Conclusions

The flaw measurement scope and definitions shown for G6-size panels were determined (excluding 15 mm for the glass edge). All measurement data have shown that this system provides stable measurement properties for α-IGZO TFT flaw pixels. This system is really suitable for the mass production of the in situ process. In the future, the system can help in improving the quality of yield required for advanced processes and production, and TFT characteristics and testing will comply with the production requirements.

An effective testing scheme was proposed by using this detection method for enhancing the inspection and testability of high-definition and small-pixel-sized TFT array panels. This testing scheme can be performed without any damage contact on the panel during the in-process inspection and detection; the in-line measurement can be conducted in real time with high capacity and stability.

Furthermore, the TFT array testing can be applied to the in-line testing of processing with TFT characterization for oxide-TFT-based and LTPS-based active matrix TFT-LCD and active matrix organic light-emitting diodes (AMOLEDs) with small-pixel-sized TFTs. It should be helpful to control the yield-in-process and reduce the manufacturing cost for advanced display applications. The results presented are useful for identifying the causes of array defects during the in-process panel testing, that is, including the critical pixel electrical leakage defect.

Acknowledgments

This work was supported by MOST of Taiwan under Contract No. MOST-110-2914-I-230-001-A1, MOST-109-2622-E-224-013 and Cheng Shiu University under Contract No. 111C03.

References

1 J.-S. Park., T.-W. Kim, D. Stryakhilev, J.-S. Lee, S.-G. An, Y.-S. Pyo, D.-B. Lee, Y. G. Mo, D.-U. Jin, and H. K. Chung: Appl. Phys. Lett. **95** (2009) 013503.
2 Y.-G. Mo, M. Kim, C. K. Kang, J. H. Jeong, Y. S. Park, C. G. Choi, H. D. Kim, and S. S. Kim: J. Soc. Inf. Disp. **19** (2011) 11.
3 W.-J. Nam, J.-S. Shim, H.-J. Shin, J.-M. Kim, W.-S. Ha, K.-H. Park, H.-G. Kim, B.-S. Kim, C.-H Oh, B.-C. Ahn, B.-C. Kim, and S.-Y. Ch: J. Soc. Inf. Disp. **44** (2013) 243.
4 Y.-C. Wang and B.-S. Lin: IEEE/ASME Trans. Mechatron. **20** (2014) 321.
5 Y.-C. Wang and B.-S. Lin: IET Sci. Meas. Technol. **8** (2014) 546.
6 Y.-M. Liu: Solid State Electron. **40** (1997) 1.

7 T. Kido, N. Kishi, and H. Takahashi: IEEE J. Sel. Top. Quantum Electron. **4** (1995) 993.
8 M. Brunner, R. Schmid, R. Schmitt, and D. Winkler: Proc. SID (1994) 755.
9 H. P. Hall and P. R. Pilotte: Proc. SID (1991) 682.
10 Y.-M. Liu: Electronic Display Forum ’95, Yokohama, Japan (1995).
11 L. C. Jenkins, R. J. Polastre, R. R. Troutman, and R. L. Wisnieff: IBM J. Res. Dev. **36** (1992) 59.
12 Y.-C. Wang and B.-S. Lin: Measurement **50** (2014) 121.
13 Y.-C. Wang and B.-S. Lin: Measurement **70** (2015) 83.